Interaction of SO_2 with Zircaloy-4 surfaces at various temperatures

N. Stojilovic and R. D. Ramsier[a)]
Departments of Physics and Chemistry, The University of Akron, Akron, Ohio 44325-4001

(Received 5 April 2006; accepted 27 June 2006; published 28 August 2006)

 [DOI: 10.1116/1.2236120]

It is known that sulfur on zirconium surfaces may delay surface oxidation[1] and reduce the sticking coefficient of adsorbing oxygen.[2] Wong and Mitchell reported that zirconium (0001) surfaces with high sulfur content do not adsorb oxygen in detectable amounts.[3] However, since zirconium in its pure form is not used in applications, it is relevant to directly investigate the surface chemistry of zirconium alloys. The origin of sulfur on Zr-alloy surfaces is often segregation from the bulk that occurs at elevated temperatures. Molecular-level understanding of the effects of sulfur on the formation and properties of protective surface oxide films is of interest, for example, in nuclear applications. Zircaloy-4 (Zry-4) is used as a structural material in water-cooled nuclear reactors at elevated temperatures, which makes our model system SO_2/Zry-4 relevant from an applied point of view.

The interaction of SO_2 with metal surfaces typically proceeds via dissociation.[4] However, in cases such as SO_2/Ag(111) (Ref. 5) or SO_2/Ag(110) (Ref. 6) molecular adsorption has been reported at low temperatures. Here, we use Auger electron spectroscopy (AES) and temperature programmed desorption (TPD) methods to study the interaction of SO_2 with surfaces of Zry-4 over a wide temperature range under ultra-high vacuum (UHV) conditions. Even though an overlap of the Zr(MNV) and S(LMM) Auger transitions makes monitoring the presence of sulfur on zirconium surfaces difficult, we show that useful information can be obtained from the Zr(MNN) and Zr(MVV) features. We also show here that H_2 desorption during TPD can occur depending on the adsorption temperature.

Experiments were performed under UHV conditions at a base pressure of about 3×10^{-10} Torr. More detailed descriptions of our UHV chamber and its pumping system are presented elsewhere.[7,8] During experiments we used an ion getter pump in combination with a titanium sublimation pump, whereas for 2 keV Ar-ion sputtering and for pumping of the gas-handling system we employed a turbomolecular pump. Gas exposures were performed with a moveable line-of-sight beam doser.[9] For collecting TPD spectra the sample was placed in line of sight to a quadrupole mass spectrometer and heated at a rate of 1.8 K/s. For AES experiments, a retarding field Auger system, operating at 3 keV, was used.

The Zry-4 sample has a thickness of 2 mm and surface area of 0.53 cm^2. The elemental composition of the sample, in weight percent, is nominally 1.2% Sn, 0.2% Fe, 0.2% Cr+O+Si, and the balance Zr. DC heating was performed via tantalum wires that are spot welded to the sample whereas cooling was carried out using a copper braid connected to a liquid-nitrogen cold finger. The sample temperature was measured via two type-E thermocouples spot welded to its sides. Cleaning of the sample was accomplished by sputtering cycles followed by annealing to about 920 K. This cleaning procedure reduces the amount of carbon and oxygen contaminants significantly, with AES peak-to-peak height ratios $C(KLL)/Zr(MNN)<0.10$ and $O(KLL)/Zr(MNN)<0.10$. We have recently shown that short annealing to 920 K does not result in significant sulfur segregation to the near-surface region of Zry-4.[10] Before adsorption experiments the [Zr(MNV)+S(LMM)]/Zr(MNN) ratio did not exceed 1.3, which according to previous studies corresponds to a sulfur-free surface.[3,11]

Figure 1(a) shows derivative mode Auger spectra of zirconium and sulfur features after cleaning and following SO_2 adsorption at 300, 600, and 900 K. The presence of sulfur in the near-surface region of Zry-4 is primarily reflected in the increased intensity of the Zr(MNV)+S(LMM) Auger feature. The formation of an oxide layer may be inferred from the shift in the Zr(MNN) transition. The vertical line near the Zr(MNN) transition is inserted to emphasize the difference for the three adsorption temperatures. The shifts in the Zr(MNN) Auger transitions imply a change in oxidation state of the surface. Note that the oxidation state following SO_2 adsorption at 900 K is the same as that of a cleaned surface implying that there is no surface oxidation. SO_2 adsorption at 300 K results in a shift of the Zr(MNN) peak by 3.0(±0.3) eV compared to the cleaned surface, whereas the feature is shifted 1.8(±0.3) eV by adsorption at 600 K. Also note that the Zr(MVV) feature is absent after SO_2 chemisorption at 300 and 600 K whereas following adsorption at 900 K it can be detected.

The Zr(MNV) feature changes in a complex way due to SO_2 adsorption, which complicates the interpretation of Fig. 1(a). The Zr(MNV) intensity appears to increase due to the presence of sulfur because of an overlap with the S(LMM) transition, but decreases due to surface oxidation by oxygen.

a)Corresponding author; electronic mail: rex@uakron.edu

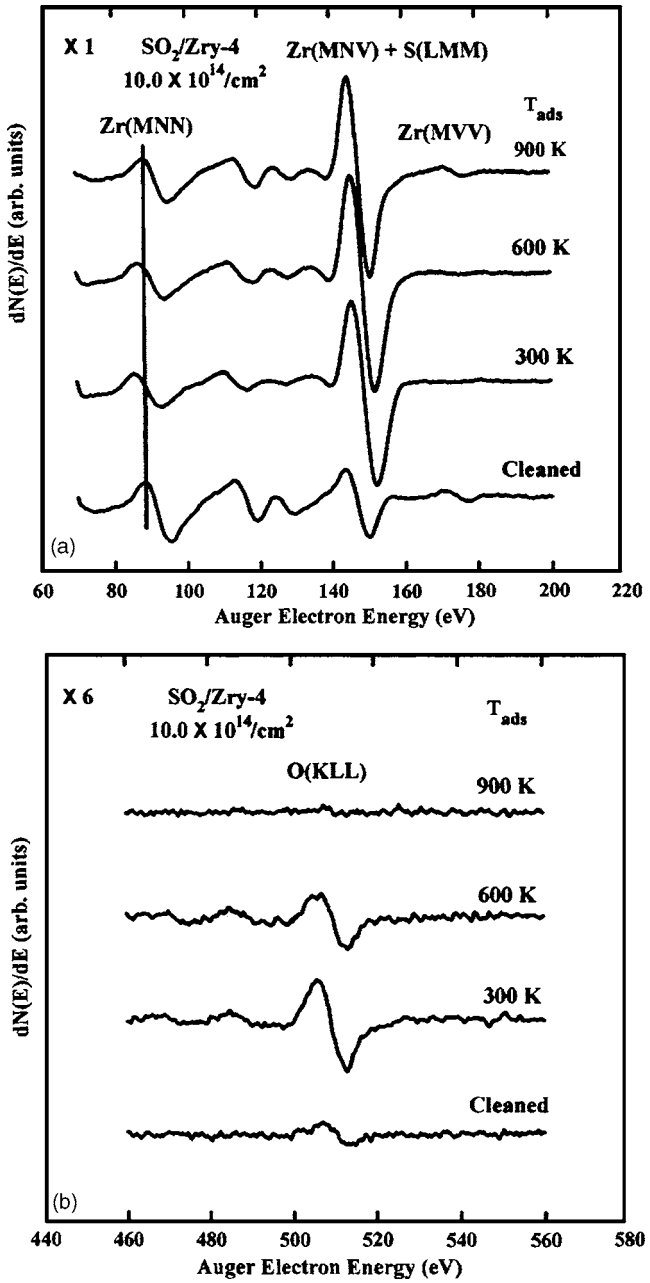

FIG. 1. Derivative mode Auger electron spectra of zirconium and sulfur features (a) and of oxygen (b), taken after cleaning the surface and after SO_2 adsorption on Zry-4 at 300, 600, and 900 K. A vertical line is inserted in (a) to indicate changes in the oxidation state of zirconium. Note that SO_2 adsorption at 300 and 600 K results in surface oxidation whereas 900 K adsorption shows no oxygen (KLL) signal and no surface oxidation. The vertical scale of panel (a) is six times larger than that of panel (b).

Thus it is desirable to consider other Zr Auger features like the Zr(MNN) transition. If we look at attenuation factors,[11] defined as $A=(I_{\text{clean}}-I_{\text{exposed}})/I_{\text{clean}}$ where "I" stands for intensity, we find that 300 and 600 K SO_2 adsorption result in the same attenuation of the Zr(MNN) feature ($A=0.38$) whereas adsorption at 900 K results in attenuation characterized by a smaller attenuation factor ($A=0.23$).

Figure 1(b) shows corresponding oxygen Auger signals. Note that the vertical scale of panel (a) is six times larger than that of panel (b). The small amount of oxygen present prior to adsorption experiments is not uncommon for zirconium-based materials that are known to be getters for oxygen. Note that after adsorption at 300 K the O(KLL) signature is the largest, consistent with the largest change in Zr oxidation state, and diminishes for higher temperatures. This is because of the faster migration of oxygen into the subsurface region at increased temperatures. The decrease in oxygen Auger signal at 600 K and its absence at 900 K cannot be attributed to a reduced sticking probability, since Fig. 1(a) indicates that a significant amount of sulfur is deposited in the near-surface region regardless of adsorption temperature. The fact that the Zr(MVV) transition can still be detected following SO_2 adsorption at 900 K [Fig. 1(a)] reveals that this transition is primarily attenuated (at 300 and 600 K) by the presence of oxygen, not sulfur.

Oxidation of Zry-4 surfaces induced by SO_2 adsorption at 300 and 600 K is interesting when one takes into account that earlier studies on pure zirconium indicated delayed surface oxidation[1] and a reduced sticking coefficient of oxygen on sulfur-rich zirconium surfaces.[2] In these two studies, O_2 adsorption on Zr(S) was investigated whereas here we observe surface oxidation by SO_2 adsorption on Zry-4. In our experiments with SO_2/Zry-4, oxygen dissolves into the bulk and no significant desorption of oxygen-containing species is observed at any temperature.

Even though AES results are often expressed in terms of Auger peak-to-peak height (APPH) ratios, due to the complicated effects of S and O on the Zr(MNV) transition one has to be careful in drawing conclusions from APPH ratios. Namely, both elements influence the intensity and shape of the Zr(MNV) feature. In order to decouple the effects of S from those of O a simple method can be used. Figure 2 shows the Zr(MNV)+S(LMM) feature following $10.0\times10^{14}/\text{cm}^2$ exposure to SO_2 and subsequent annealing to 900 K when no oxygen signal is observed in AES. Since we did not observe the desorption of sulfur-containing species in TPD, and since diffusion of sulfur into the bulk is not expected, the removal of oxygen from the region probed by AES results in decoupling the O and S effects on the Zr(MNV) transition. Note that the intensities of the zirconium Auger features are notably increased following removal of oxygen from the near-surface region. Although AES data typically do not directly reveal oxidation state information, the shift of the Zr(MNN) peak toward higher kinetic energies indicates a change in the oxidation state of Zr.

Figure 3(a) shows the [Zr(MNV)+S(LMM)]/Zr(MNN) Auger peak-to-peak ratio as a function of SO_2 exposure at 300, 600, and 900 K. Even though the Zr(MNV) feature changes shape due to the presence of oxygen, its intensity is mainly affected by sulfur at the higher temperatures, so we can justify using APPH ratios in this case. The figure indicates that SO_2 adsorption at 900 K results in relatively rapid saturation of the amount of sulfur at the surface compared to adsorption at 300 and 600 K. We propose that this saturation of the sulfur Auger signal at 900 K indicates that there is no further adsorption of SO_2 above an exposure of about

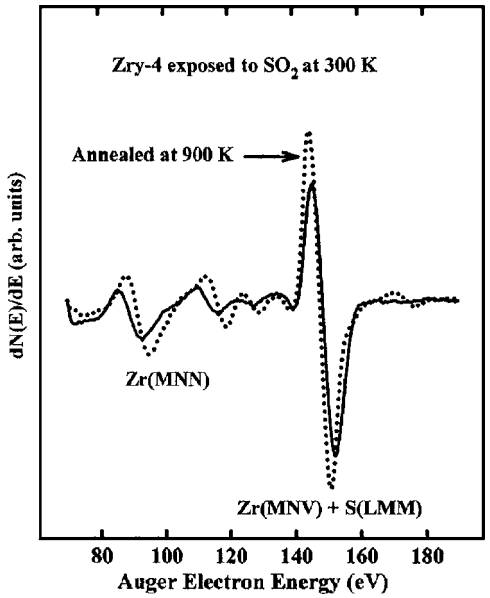

FIG. 2. Derivative mode Auger electron spectra of zirconium and sulfur features following SO_2 adsorption of $10.0\times10^{14}/cm^2$ on Zry-4 at 300 K (solid line), and following annealing to 900 K when no oxygen signal is detected in AES (dotted line). Since sulfur remains near the surface following annealing the figure shows how the effects of S and O on the Zr(MNV) feature can be decoupled.

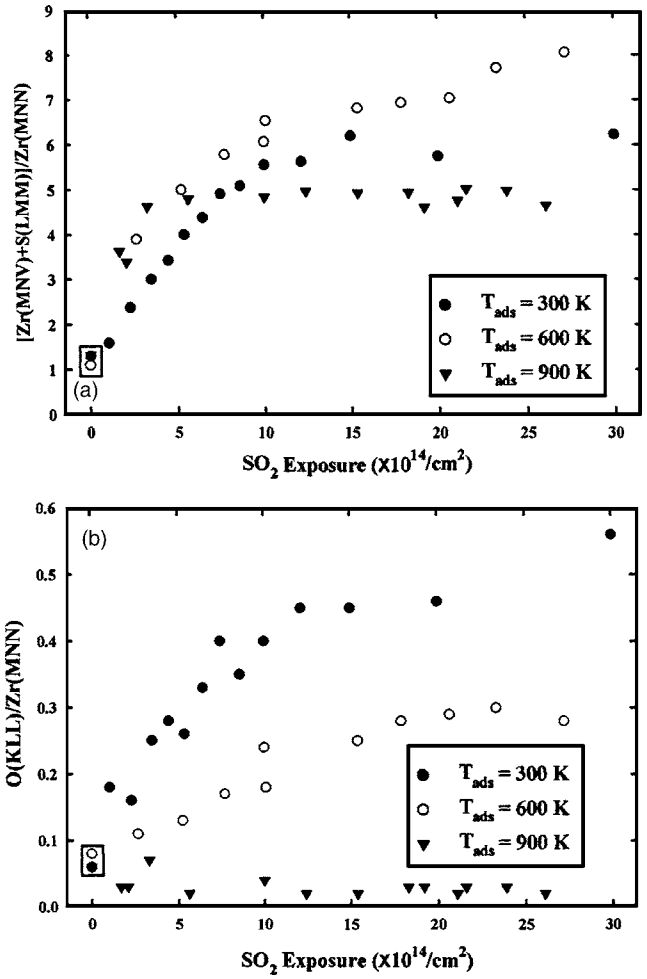

FIG. 3. [Zr(MNV)+S(LMM)]/Zr(MNN) (a) and O(KLL)/Zr(MNN) (b) Auger peak-to-peak height ratios versus SO_2 exposure at 300, 600, and 900 K. The oxygen Auger signal is near the detection limit after 900 K adsorption. Note the difference in both sulfur and oxygen content in all three cases. Boxes enclosing data points before exposure indicate uncertainties in achieving clean surfaces. Data points for all three adsorption temperatures are obtained from several independent measurements to ensure the reproducibility of trends.

$5.0\times10^{14}/cm^2$. In addition, a greater sulfur Auger signal is observed following exposure to SO_2 at 300 and 600 K than after adsorption at 900 K. What is interesting is that Zry-4 surfaces at 900 K rapidly adsorb sulfur dioxide at relatively low exposures, keeping the sulfur near the surface and with oxygen probably dissolving into the bulk.

Adsorption at 600 K results in the greatest [Zr(MNV) +S(LMM)]/Zr(MNN) ratio up to exposures of 30.0×10^{14} cm^2. This does not mean that there is more sulfur deposited by adsorption at 600 K than at 300 K. Remember that at 300 K, as Fig. 2 shows, oxygen has a notable effect on the Zr(MNV)+S(LMM) feature, which was not observed at 600 or 900 K. In other words, the presence of oxygen in the surface region at 300 K reduces the sulfur Auger signal by shielding or site blocking and affects the Zr Auger electrons originating from the MNV transition.

Figure 3(b) shows corresponding O(KLL)/Zr(MNN) ratios as a function of SO_2 exposure and demonstrates that there is a significant difference in the oxygen content in the near-surface region of Zry-4 at these three temperatures. The oxygen deposited on the surface following SO_2 adsorption dissolves into the substrate, and this process dominates at higher temperatures, in agreement with the literature.[11] Even though we cannot rule out the desorption of molecular O_2 *during* SO_2 adsorption, this process is unlikely due to the high affinity of zirconium for oxygen. However, it is apparent that SO_2 does adsorb, even at 900 K, and deposits sulfur near the surface. Note that more oxygen resides near the surface following SO_2 adsorption at 300 K than at 600 K whereas the sulfur content in Fig. 3(a) shows an opposite trend. Again, this does not necessarily mean that there is less oxygen deposited at 600 K but rather that oxygen penetrates deeper into the subsurface at this temperature leaving the sulfur to cover the surface. Showing AES data in terms of the APPH ratios indicates that oxygen at 300 K at least partly covers sulfur, whereas at 600 K it penetrates deeper into the subsurface region and shows no significant effect on the Zr(MNV)+S(LMM) signal intensity. Data points in all three cases have been obtained from several independent measurements to ensure the reproducibility of trends.

TPD data provide no evidence of molecular desorption following exposure of Zry-4 surfaces to SO_2 regardless of adsorption temperature. This is consistent with our earlier study of SO_2 adsorption on Zr(0001) at 150 K.[12] However, here we observe hydrogen desorption that depends on adsorption temperature. Figure 4 shows hydrogen (H_2) TPD profiles following SO_2 exposures of $15.0\times10^{14}/cm^2$ at 300, 600, and 900 K. Note that the most pronounced hydrogen peak is observed following SO_2 adsorption at 600 K where

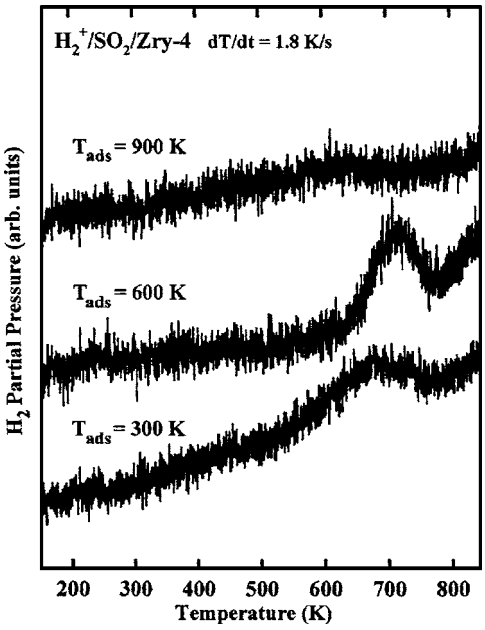

FIG. 4. H_2 partial pressure (2 amu) as a function of temperature following SO_2 adsorption ($15.0\times10^{14}/cm^2$) at 300, 600, and 900 K. Following exposure to SO_2 the surface was cooled to about 150 K in all three cases and the spectra were then collected while heating at a rate of 1.8 K/s.

the surface holds the largest amount of sulfur. Based on the fact that oxygen is known to attract hydrogen from the substrate,[13,14] one may expect the greatest hydrogen desorption signal after SO_2 adsorption at 300 K, as this is the surface with the most oxygen [Fig. 3(b)].

At 600 K, based on the AES results, oxygen penetrates deeper into the substrate leaving sulfur at the surface. However, sulfur may also attract hydrogen, and it is unclear as to which effect may dominate. It is therefore likely that the oxidation state of the surface and the amount of sulfur both play important role(s) in hydrogen interactions and the subsequent desorption of hydrogen. Since the hydrogen desorption signals are relatively small, our TPD results are more interesting from the fundamental than from the applied point of view.

SO_2 adsorbs on surfaces of Zry-4 in a wide temperature range. Interestingly, even hot Zry-4 surfaces readily adsorb sulfur dioxide. Adsorption of SO_2 at 300 and 600 K results in the formation of an oxide layer, as observed by shifts in the Zr(MNN) feature, whereas adsorption at 900 K shows no oxygen Auger signal nor evidence for surface oxide. Decreases in the O(KLL) feature with increasing temperature can be explained by faster O migration into the bulk of Zry-4 at higher temperatures.[11] Even though higher exposures to SO_2 exhibit the greatest Zr(MNV)+S(LMM) feature following adsorption at 600 K, this is because oxygen diffuses faster at higher temperatures and occupies sites beneath sulfur. We observe hydrogen desorption near 700 K that is most pronounced following SO_2 adsorption at 600 K, where we propose that more sulfur resides closer to the surface. This observation is relevant in the context of recent work on the same alloy where we have shown that this hydrogen TPD feature is also induced by oxygen adsorption.[15] Even though the origin of this hydrogen desorption state is difficult to prove, we observe that it not only depends on the presence of oxygen but also strongly depends on adsorption temperature.

We would like to thank Wah Chang for providing the Zry-4 material used in this study, and we acknowledge a grant from NIH-NIBIB, No. EB003397-01, which supports some of our work on zirconium alloys. The authors are grateful to an anonymous referee for a thorough review and good suggestions for improving this manuscript.

[1]T. Tanabe and M. Tomita, Surf. Sci. **220**, 333 (1989).
[2]K. Ojima and K. Ueda, Appl. Surf. Sci. **165**, 141 (2000).
[3]P. C. Wong and K. A. R. Mitchell, Can. J. Chem. **64**, 2409 (1986).
[4]J. Haase, J. Phys.: Condens. Matter **9**, 3647 (1997).
[5]M. E. Castro and J. M. White, J. Chem. Phys. **95**, 6057 (1991).
[6]D. A. Outka and R. J. Madix, Surf. Sci. **137**, 242 (1984).
[7]Y. C. Kang, M. M. Milovancev, D. A. Clauss, M. A. Lange, and R. D. Ramsier, J. Nucl. Mater. **281**, 57 (2000).
[8]Y. C. Kang and R. D. Ramsier, J. Nucl. Mater. **303**, 125 (2002).
[9]N. Stojilovic, J. C. Tokash, and R. D. Ramsier, Surf. Sci. **565**, 243 (2004).
[10]N. Stojilovic, E. T. Bender, and R. D. Ramsier, Appl. Surf. Sci. **252**, 1806 (2005).
[11]J. S. Foord, P. J. Goddard, and R. M. Lambert, Surf. Sci. **94**, 339 (1980).
[12]N. Stojilovic, J. C. Tokash, and R. D. Ramsier, Surf. Sci. **553**, 23 (2004).
[13]D. A. Asbury, G. B. Hoflund, W. J. Peterson, R. E. Gilbert, and R. A. Outlaw, Surf. Sci. **185**, 213 (1987).
[14]W. F. Peterson, R. E. Gilbert, and G. B. Hoflund, Appl. Surf. Sci. **24**, 121 (1985).
[15]N. Stojilovic, E. T. Bender, and R. D. Ramsier, J. Nucl. Mater. **348**, 79 (2006).